Monthly Notices
of the
ROYAL ASTRONOMICAL SOCIETY

MNRAS **461,** L41–L45 (2016)
Advance Access publication 2016 May 10

doi:10.1093/mnrasl/slw093

Probing the early chemical evolution of the Sculptor dSph with purely old stellar tracers

C. E. Martínez-Vázquez,[1,2]★ M. Monelli,[1,2]★ C. Gallart,[1,2] G. Bono,[3,4] E. J. Bernard,[5] P. B. Stetson,[6] I. Ferraro,[4] A. R. Walker,[7] M. Dall'Ora,[8] G. Fiorentino[9] and G. Iannicola[4]

[1]*Instituto de Astrofísica de Canarias (IAC), E-38205 La Laguna, Tenerife, Spain*
[2]*Dpto. Astrofísica, Universidad de La Laguna (ULL), E-38206 La Laguna, Tenerife, Spain*
[3]*Dipartimento di Fisica, Università di Roma Tor Vergata, Via della Ricerca Scientifca 1, I-00133 Roma, Italy*
[4]*INAF-Osservatorio Astronomico di Roma, Via Frascati 33, I-00040 Monteporzio Catone, Italy*
[5]*Laboratoire Lagrange, Observatoire de la Côte d'Azur, F-06304 Nice Cedex 4, France*
[6]*Herzberg Astronomy and Astrophysics, National Research Council Canada, 5071 West Saanich Road, Victoria, BC V9E 2E7, Canada*
[7]*Cerro Tololo Inter-American Observatory, National Optical Astronomy Observatory, Casilla 603, La Serena, Chile*
[8]*INAF-Osservatorio Astronomico di Capodimonte, Via Moiariello 16, I-80131 Napoli, Italy*
[9]*INAF-Osservatorio Astronomico di Bologna, via Ranzani 1, I-40127, Bologna, Italy*

Accepted 2016 May 6. Received 2016 May 6; in original form 2016 April 14

ABSTRACT

We present the metallicity distribution of a sample of 471 RR Lyrae (RRL) stars in the Sculptor dSph, obtained from the *I*-band period–luminosity relation. It is the first time that the early chemical evolution of a dwarf galaxy is characterized in such a detailed and quantitative way, using photometric data alone. We find a broad metallicity distribution (full width at half-maximum equals to 0.8 dex) that is peaked at [Fe/H] $\simeq -1.90$ dex, in excellent agreement with literature values obtained from spectroscopic data. Moreover, we are able to directly trace the metallicity gradient out to a radius of ∼55 arcmin. We find that in the outer regions ($r >$ ∼32 arcmin) the slope of the metallicity gradient from the RRLs (-0.025 dex arcmin^{-1}) is comparable to the literature values based on red giant (RG) stars. However, in the central part of Sculptor, we do not observe the latter gradients. This suggests that there is a more metal-rich and/or younger population in Sculptor that does not produce RRLs. This scenario is strengthened by the observation of a metal-rich peak in the metallicity distribution of RG stars by other authors, which is not present in the metallicity distribution of the RRLs within the same central area.

Key words: stars: variables: RR Lyrae – galaxies: evolution – galaxies: individual: Sculptor dSph – Local Group – galaxies: stellar content.

1 INTRODUCTION

RR Lyrae (RRL) stars are low-mass, core helium burning, radially pulsating stars. They are primary distance indicators, since they obey well-defined optical/near-infrared period–luminosity (PL) relations. They are relatively bright and can currently be observed out to ∼2 Mpc (Da Costa et al. 2010; Yang et al. 2014). They are also firm tracers of old (>10 Gyr) stellar populations, and can be used to constrain the early evolution of the host stellar systems (Bernard et al. 2008). In particular, their pulsation properties are tightly connected with the metallicity distribution of their parent stellar populations (see e.g. Bono et al. 2011, for a review).

Several theoretical and empirical investigations have focused on the use of pulsation properties to constrain the RRL metal content. The most popular are Fourier decomposition parameters (such as ϕ_{31} among others, see e.g. Nemec et al. 2013, and references therein) and the combination of luminosity, period, and amplitude (see section 5 of Jeffery et al. 2011, for a detailed review). Recently, Marconi et al. (2015) presented a new comprehensive theoretical framework for RRL stars including a broad range in stellar masses, luminosities and chemical compositions. They provided new optical and near-infrared period–luminosity–metallicity (PLZ) and period–Wesenheit–metallicity (PWZ) relations with various degrees of metallicity dependence. In this investigation, we take advantage of the *I*-band PLZ relation to evaluate the metallicity of individual Sculptor RRL stars, thus constraining its early chemical evolution.

★ E-mail: clara.marvaz@gmail.com (CEM-V); monelli@iac.es (MM)

Sculptor is a gold mine for understanding galaxy evolution, since it is relatively close to the Milky Way ($\mu = 19.62$ mag; Martínez-Vázquez et al. 2015, hereafter Paper I), and is the crossroads of several theoretical (e.g. Romano & Starkenburg 2013; Salaris et al. 2013), photometric (e.g. Da Costa 1984; Kaluzny et al. 1995; Hurley-Keller, Mateo & Grebel 1999; Majewski et al. 1999; Monkiewicz et al. 1999; Harbeck et al. 2001; de Boer et al. 2011, 2012, Paper I) and spectroscopic investigations (e.g. Tolstoy et al. 2004; Clementini et al. 2005; Battaglia et al. 2008; Walker, Mateo & Olszewski 2008; Kirby et al. 2009; Starkenburg et al. 2013; Skúladóttir et al. 2015). Sculptor is a low-mass dwarf galaxy whose stellar populations display a relatively narrow age range, but still it is a quite complex system in its structure and chemical enrichment.

The current sample of RRL stars was discussed by Martínez-Vázquez et al. (2016), based on a photometric (*BVI*) catalogue covering a time interval of ∼24 yr and including 536 RRL stars (289 RRab, fundamental; 197 RRc, first overtone; 50 RRd, double mode).

2 METALLICITY DISTRIBUTION

Recent theoretical (Marconi et al. 2015) and empirical studies (Braga et al. 2016) indicate that the *I*-band PLZ relation (*I*-PLZ) is a reliable diagnostic to derive the metallicity of individual RRLs. By inverting the *I*-PLZ relation, we obtain

$$[\mathrm{Fe/H}] = \frac{M_I - b \log P - a}{c}, \quad (1)$$

where the coefficients a, b and c are listed in table 6 of Marconi et al. (2015). We use here the absolute M_I magnitudes for a reddening $E(B-V) = 0.018$ mag (Pietrzynski et al. 2008) and the RRL distance modulus (19.62 mag) derived in Paper I from the metal-independent PW relations. Note that we use *I*-PLZ relations for RRab and RRc variables separately, since they have slightly different slopes. To illustrate the reliability of the method and provide an empirical estimate of the uncertainty on the inferred metallicities, we applied it to the RRLs of the globular cluster Reticulum, which have accurate light curves (Kuehn et al. 2013), low reddening ($E(B-V) = 0.016$ mag; Schlegel, Finkbeiner & Davis 1998), and metallicity ([Fe/H] $= -1.61 \pm 0.15$ – Mackey & Gilmore 2004 – on the Carretta et al. 2009 scale) close to that of Sculptor. Applying equation (1) to the corresponding pulsational properties of 22 RRab+RRc stars in Reticulum (excluding Blazhko and multimode RRLs), we obtain a mean metallicity of −1.49 dex and $\sigma = 0.25$ dex. Since there is no (known) metallicity spread in this cluster, the σ is a representative of the uncertainty of the technique. In fact, by selecting the best quality light curves (11), we improve on these results, obtaining a mean metallicity of −1.60 dex and $\sigma = 0.07$ dex.

The black histogram in Fig. 1 shows the metallicity distribution based on the full RRL sample (471 RRab+RRc), while the grey-filled red one is for the clean sample (290 RRLs with well sampled and accurate light curves, see Paper I for a detailed discussion concerning sample selection). We fit Gaussian curves to the metallicity distributions (dashed curves), and found that the peak and the σ of the two distributions are consistent. Therefore, the full RRL sample is adopted in the following analysis.

Fig. 1 shows that the metallicity distribution of the Sculptor RRL stars peaks at [Fe/H] $= -1.90$ with $\sigma = 0.35$ dex, and a total range in metallicity of the order of 2 dex. However, the metal-poor and the metal-rich tails of the distribution should be treated cautiously since metallicity estimates are based on a photometric

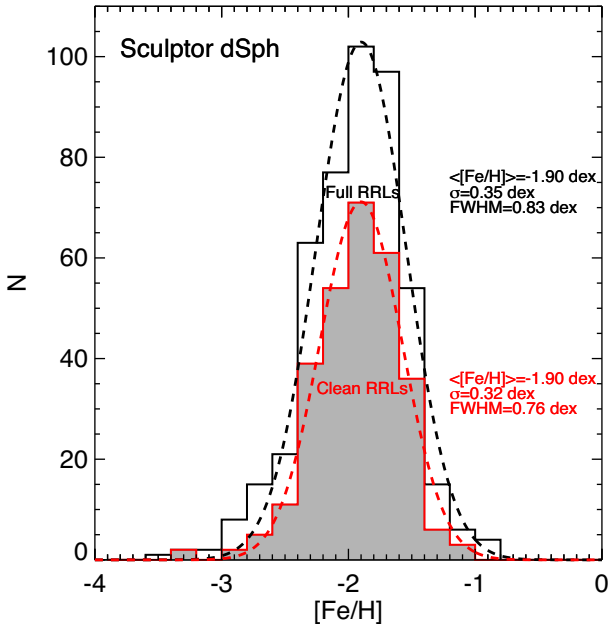

Figure 1. Metallicity distribution based on the *I*-PLZ relation for the full (black) and the clean (red and grey filled) samples of RRL stars. The peaks agree well with literature values.

index. Using the value of σ obtained in Reticulum as an estimate of the dispersion of this method, we find that the intrinsic metallicity spread is $\sigma \sim 0.25$ dex. On the other hand, we note that recent spectroscopic investigations in Sculptor have found both very metal poor red giant (RG) stars ([Fe/H] < -3.0, Tafelmeyer et al. 2010; Starkenburg et al. 2013), and RG stars with [Fe/H] ~ -1.0 (Kirby et al. 2009).

Fig. 2 compares spectroscopic metallicity estimates available in the literature. In the left-hand panel, the metallicity distribution based on the *I*-PLZ relation (black) is compared to the RRL metallicities from Clementini et al. (2005, magenta curves), using a revision of the ΔS method (quoted individual errors ≈ ±0.15–0.16 dex); we show only the 98 RRab+RRc variables in common. For a detailed comparison, both metallicity distributions were converted to the homogeneous metallicity scale of Carretta et al. (2009). The peaks and σ's of the two metallicity distributions are indistinguishable; the agreement between the two methods is excellent.

The middle panel shows that the agreement remains good if we compare our metallicity distribution with the sizeable sample (513 RG stars) of spectroscopic measurements provided by Helmi et al. (2006, red histogram). The latter employ low-resolution spectra of the Ca II triplet as a metallicity diagnostic (quoted error ≈ ±0.1 dex). Note that the spatial distribution of their RG stars and our RRL stars is similar: both include stars out to a radius of ∼60 arcmin, near the tidal radius of Sculptor. The two metallicity distributions are quite symmetric and consistent.

Finally, the right-hand panel of Fig. 2 compares the metallicity distribution of our RRL sample with that of the RG stars provided by Kirby et al. (2009, green histogram) from medium-resolution spectra (quoted error ≈ ±0.15). To limit any bias due to the metallicity gradient (see Section 3), the comparison used the RRL and RG stars located in the region ($r < 9.5$ arcmin) homogeneously covered by the spectroscopic observations. A glance at the histograms plotted here indicates that the RG sample contains a metal-rich component not represented in the RRL sample; this component is not

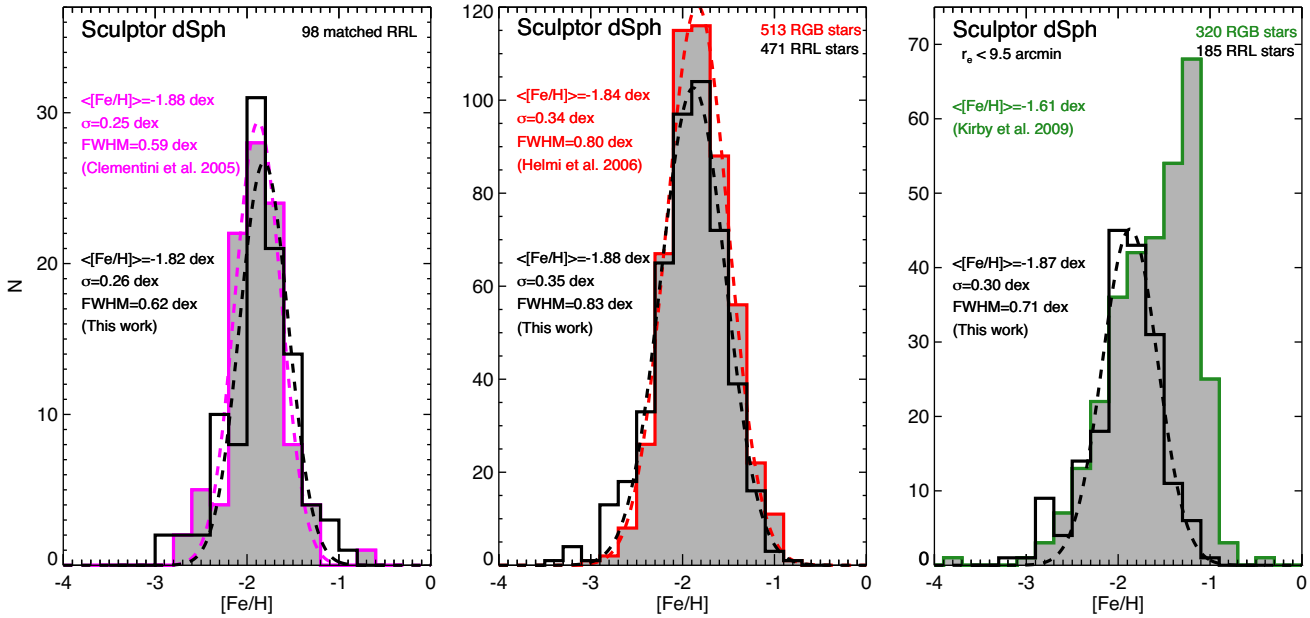

Figure 2. Comparison of the derived metallicity distribution with spectroscopic data available in the literature. Left-hand panel: the 98 RRL stars in common between our sample (black histogram) and that of Clementini et al. (2005, magenta histogram), who obtained the abundances using the ΔS method. Middle panel: our full RRL sample (black histogram) versus the 513 red giant (RG) stars provided by Helmi et al. (2006), using the Ca II triplet. Right-hand panel: our RRL stars within 9.5 arcmin versus the RG stars provided by Kirby et al. (2009) in the same area. Note that the above metallicity distributions assume the same solar iron abundance (log ϵ(Fe) = 7.52).

obvious in the more spatially extended sample of RG from Helmi et al. (2006), as already noted by Kirby et al. (2009). Interestingly, the RRL metallicity distribution does not seem to show significant differences between the sample in the innermost region and that covering the entire galaxy.

The difference between the metallicity distributions of the RRL and RG stars in the centre of Sculptor may be explained by evolutionary effects: as the iron abundance increases, the horizontal branch (HB) morphology becomes redder, until the RRL instability strip is no longer populated (Fiorentino et al. 2012). Age has a similar effect, with younger populations also having a redder HB. This is why the metal-rich globular clusters and younger, outer-halo clusters display a stub of HB red stars and very few, if any, RRL stars. This interpretation is supported by the clear difference in radial distribution between red and blue HB stars discussed in Paper I.

3 THE RADIAL METALLICITY GRADIENTS OF THE RRL STARS IN SCULPTOR

In Paper I, we showed that Sculptor RRLs have a spread in V magnitude of ∼0.35 mag, significantly larger than the uncertainties in the mean magnitudes of individual variables ($\sigma = 0.03$ mag), and also significantly larger than the spread expected from evolution in a mono-metallic stellar population. We associated the bright (Bt) RRL sample with the more metal-poor stellar population, and the faint (Ft) sample with a metal-rich one.

Fig. 3 shows the $\langle V\rangle$-band luminosity function for our 471 RRL stars (blue histogram). The green curves represent the three Gaussian components adopted to describe the magnitude distribution, while the red curve is the sum of the three Gaussians. There are two prominent peaks at $\langle V\rangle \sim 20.12$ and $\langle V\rangle \sim 20.19$. We adopt the local minimum at $\langle V\rangle = 20.155$ (purple vertical dashed line) to split the RRL sample into Bt and Ft subsamples (Paper I).

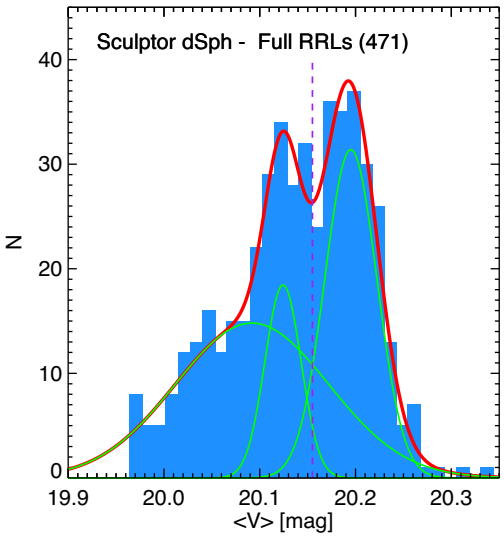

Figure 3. $\langle V\rangle$-band luminosity function for our RRL sample. The green curves display the three individual Gaussians adopted to fit the magnitude distribution, while the red curve is the convolution of the three Gaussians. The purple vertical dashed line marks the luminosity level adopted to separate Bt and Ft RRLs.

Taking advantage of the new metallicity determinations, we investigate the difference in metallicity between the two sub-populations. As expected, the Bt sub-sample is, on average, more metal poor than the Ft one. A Gaussian fit to the metallicity distribution of each sample discloses that the two distributions have similar σ's ($\sigma_{\rm Bt} = 0.29$ dex, $\sigma_{\rm Ft} = 0.32$ dex) and partially overlap, but the difference in the mean metallicity ([Fe/H] = −2.03 [Bt] versus [Fe/H] = −1.74 [Ft]), of the order of 1σ (0.3 dex), robustly indicates the presence of two sub-populations. In Paper I, we showed that the

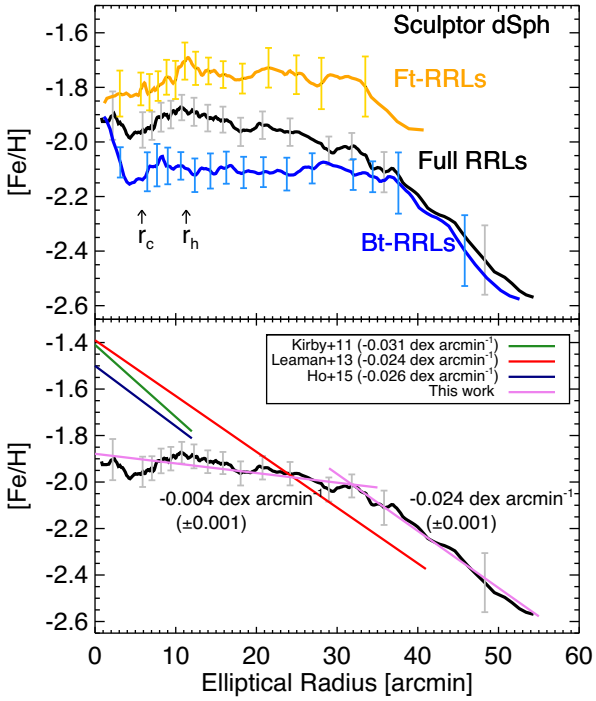

Figure 4. Top: metallicity distribution as a function of the elliptical radius for the full sample of RRLs (black), Bt-RRLs (blue), and Ft-RRLs (orange). The vertical arrows mark the core (r_c = 5.8 arcmin, Mateo 1998) and the half-light radius (r_h = 11.3 arcmin; Irwin & Hatzidimitriou 1995). The vertical bars display the errors on [Fe/H] based on Monte Carlo simulations. Bottom: comparison with the radial spectroscopic gradients measured by Kirby et al. (2011, green), Leaman et al. (2013, red), and Ho et al. (2015, dark blue). The current and the literature slopes are also labelled.

Bt and Ft samples follow different spatial distributions, with the Ft RRLs more centrally concentrated than the Bt ones, suggesting the presence of a metallicity gradient. Tolstoy et al. (2004) reached a similar conclusion from the spatial distribution of red and blue HB stars.

Our individual metallicities also allow us to measure the radial metallicity profile of the oldest stellar population in Sculptor. The top panel of Fig. 4 shows the metallicity of the Bt (blue), Ft (orange) and global (black) RRL samples as a function of the elliptical radius. The metallicity of the Bt sub-sample remains constant, within the errors, over a substantial fraction of the body of the galaxy ($r \sim$ 30 arcmin) – the peak in the centre is not significant as shown by the single error bar. At larger radii, the profile shows a steady decrease and approaches a metallicity $\sim$−2.5 dex in the outskirts of the galaxy ($r \sim$ 50 arcmin). The radial trend of the Ft sub-group is consistent with a constant metallicity ([Fe/H] ~ -1.75), although there is a hint of a lower metallicity within the half-light radius (r_h = 11.3 arcmin). The metallicity decrease of the global sample beyond $\sim$35 arcmin is significant, though the error bars are larger due to the smaller number of RRL stars in the last radial bins. Interestingly, the metallicity of the global sample also shows a mild gradient within $\sim$25 arcmin, where the sub-samples are flat; this is due to the varying ratio of Bt and Ft as a function of radius.

To characterize the change in iron abundance as a function of radius, more quantitatively, we fit the gradient with two linear relations: the violet lines plotted in the bottom panel of Fig. 4 show the fit for radial distances smaller and larger than $r \sim$ 32 arcmin. We find that the metallicity profile in the inner region has a mild negative slope (-0.004 ± 0.001 dex arcmin^{-1}), while the outermost region displays a well-defined gradient with a steeper negative slope (-0.025 ± 0.001 dex arcmin^{-1}).

The RRL metallicity gradient of the outermost regions agrees quite well with the RG metallicity gradient found by Leaman et al. (2013) from low-resolution spectra collected by Tolstoy et al. (2004). Their sample covers a significant fraction of the galaxy and yields a gradient of -0.14 ± 0.02 dex/r_c [-0.024 dex arcmin^{-1}, assuming, r_c equals to 5.8 arcmin (Mateo 1998) – see the red line in the bottom panel of Fig. 4]. However, the quoted gradient is systematically steeper than that derived here for radii smaller than 25 arcmin. In fact, the constant slope of -0.024 dex arcmin^{-1} quoted by Leaman et al. (2013), implies a central metallicity of -1.4 dex, compared with the -1.9 dex for the average metallicity of the RRL stars. This evidence further supports the difference between the metallicity distribution of purely old (RRLs) and possibly mixed-age (RG) stellar tracers discussed in Section 2.

The same conclusion applies to the metallicity gradient estimated by Kirby et al. (2011) of -0.18 ± 0.02 dex/r_c (-0.031 dex arcmin^{-1}), but the range in radii covered by these data is quite limited ($\sim$2 r_c, $\sim$12 arcmin). Using the same spectra, but a different calibration for the Ca II triplet, Ho et al. (2015) found a slightly shallower slope: -0.293 ± 0.025 dex/r_h (-0.026 dex arcmin^{-1}).

We have already mentioned that the current data do not allow us to constrain whether the lack of metal-rich RRL (as metal-rich as the metal-rich RG from Kirby et al. 2009) is a consequence of these stars being too metal-rich, too young, or both, since the effect is the same: the HB is too red to put stars in the instability strip. However, the metallicity gradient in the RRL indicates that the outermost region in Sculptor is dominated by an old stellar population that is more metal poor than the old stellar population in the innermost regions. This implies a larger chemical enrichment in the inner region (by $\sim$0.5 dex) during the period when the stellar population producing the RRL stars was formed. The above results also suggest that there is an additional stellar population located in the innermost regions that experienced additional enrichment, causing a drift of the mean metallicity into the metal-intermediate regime ([Fe/H] $\gtrsim -1.5$). Under the assumption of continuous metal enrichment, this could be a younger population that has no RRL counterpart. This suggests that star formation and in turn, chemical enrichment lasted longer in the centre of Sculptor than in the outermost regions.

4 FINAL REMARKS

We investigated the metallicity distribution of a sample of 471 RRL stars in the Sculptor dSph galaxy, based on the *I*-PLZ relation. The RRL stars cover a broad range in metallicity ($\sim$2.0 dex), confirming previous suggestions of efficient early chemical enrichment in the oldest stellar population in Sculptor. We have shown that RRL stars trace a well-defined radial metallicity gradient, shallow within 32 arcmin but much steeper beyond that.

In particular, we found that in the outer regions ($r \gtrsim$ 32 arcmin), the slope of the metallicity gradient from our RRL sample (-0.025 dex arcmin^{-1}) is almost the same as the slope derived by Leaman et al. (2013), who studied RG stars out to large galactocentric radius. However, in the central part ($r \lesssim$ 32 arcmin), we do not observe the steep gradients found from spectra of RG stars. The gradient in the RRL sample (-0.004 dex arcmin^{-1}) is significantly shallower than the literature values for RGs in the same region (Kirby et al. 2011; Leaman et al. 2013; Ho et al. 2015). This

suggests that there is a metal-rich and/or younger population in the centre of Sculptor that does not have a counterpart among the RRLs. This scenario is supported by a metal-rich peak in the metallicity distribution of RG stars (Kirby et al. 2009) that is not present in the metallicity distribution of the RRLs (inside the same area, $r_e < 9.5$ arcmin).

We have presented a powerful new method, from the inverse of the *I*-PLZ relation, for studying the internal characteristics of old stellar populations in galaxies. The different metallicity profiles of the RRL and RG stars in Sculptor reveal a general outside-in formation scenario routinely found in dwarf galaxies (Harbeck et al. 2001; Stinson et al. 2006; Hidalgo et al. 2013), but are able to more narrowly delimit the successive stellar generations in space and time. Beyond ≈32 arcmin ($5.5 \times r_c$) from the centre, the RG and RRL appear to define a uniform population in terms of age and metallicity. Conversely, inside this radius we find solid indications that the RG population is progressively more metal rich and/or younger towards the centre of the galaxy. Under the reasonable assumption of a monotonic increase of metallicity with time, this indicates a more extended period of star formation towards the centre of Sculptor. Star formation must have ended around 10 Gyr ago (the minimum age canonically adopted for RRL stars) beyond a radius of ≈32 arcmin. Inside this radius, it continued for some time, with younger stars becoming progressively more chemically enriched (by up to ∼0.5 dex). This scenario agrees with the spatially resolved star formation rate obtained by de Boer et al. (2012) from a colour–magnitude diagram reaching the oldest main-sequence turn-offs (MSTOs). This shows that RRL stars can provide detailed information on the oldest population of a galaxy in the absence of old MSTO photometry. In particular, by combining RRL and RG metallicities and metallicity profiles, we are able to identify a characteristic radius beyond which the stellar population is purely old (>10 Gyr) and inside which star formation and chemical enrichment proceeded for a longer period of time. To quantify the extension of this period to younger ages, the red-HB and red-clump morphology can provide some further insight. However, MSTO information is still the best bet for accurate ages.

ACKNOWLEDGEMENTS

The authors thank the anonymous referee for the useful comments. This research has been supported by the Spanish Ministry of Economy and Competitiveness (MINECO) under the grant (project reference AYA2014-56795-P). EJB acknowledges support from the CNES postdoctoral fellowship program. GF has been supported by the Futuro in Ricerca 2013 (grant RBFR13J716).

REFERENCES

Battaglia G., Irwin M., Tolstoy E., Hill V., Helmi A., Letarte B., Jablonka P., 2008, MNRAS, 383, 183
Bernard E. J. et al., 2008, ApJ, 678, L21
Bono G., Dall'Ora M., Caputo F., Coppola G., Genovali K., Marconi M., Piersimoni A. M., Stellingwerf R. F., 2011, in McWilliam A., ed., RR Lyrae Stars, Metal-Poor Stars, and the Galaxy. The Observatories of the Carnegie Institution of Washington, Pasadena, CA, p. 1
Braga V. F. et al., 2016, A&A, submitted
Carretta E., Bragaglia A., Gratton R., D'Orazi V., Lucatello S., 2009, A&A, 508, 695
Clementini G., Ripepi V., Bragaglia A., Martinez Fiorenzano A. F., Held E. V., Gratton R. G., 2005, MNRAS, 363, 734
L.de Boer T. J. et al., 2011, A&A, 528, A119
L.de Boer T. J. et al., 2012, A&A, 539, A103
Da Costa G. S., 1984, ApJ, 285, 483
Da Costa G. S., Rejkuba M., Jerjen H., Grebel E. K., 2010, ApJ, 708, L121
Fiorentino G., Stetson P. B., Monelli M., Bono G., Bernard E. J., Pietrinferni A., 2012, ApJ, 759, L12
Harbeck D. et al., 2001, AJ, 122, 3092
Helmi A. et al., 2006, ApJ, 651, L121
Hidalgo S. L. et al., 2013, ApJ, 778, 103
Ho N., Geha M., Tollerud E. J., Zinn R., Guhathakurta P., Vargas L. C., 2015, ApJ, 798, 77
Hurley-Keller D., Mateo M., Grebel E. K., 1999, ApJ, 523, L25
Irwin M., Hatzidimitriou D., 1995, MNRAS, 277, 1354
Jeffery E. J. et al., 2011, AJ, 141, 171
Kaluzny J., Kubiak M., Szymanski M., Udalski A., Krzeminski W., Mateo M., 1995, A&AS, 112, 407
Kirby E. N., Guhathakurta P., Bolte M., Sneden C., Geha M. C., 2009, ApJ, 705, 328
Kirby E. N., Lanfranchi G. A., Simon J. D., Cohen J. G., Guhathakurta P., 2011, ApJ, 727, 78
Kuehn C. A. et al., 2013, AJ, 145, 160
Leaman R. et al., 2013, ApJ, 767, 131
Mackey A. D., Gilmore G. F., 2004, MNRAS, 352, 153
Majewski S. R., Siegel M. H., Patterson R. J., Rood R. T., 1999, ApJ, 520, L33
Marconi M. et al., 2015, ApJ, 808, 50
Martínez-Vázquez C. E. et al., 2015, MNRAS, 454, 1509 (Paper I)
Martínez-Vázquez C. E. et al., 2016, MNRAS, submitted
Mateo M. L., 1998, ARA&A, 36, 435
Monkiewicz J. et al., 1999, PASP, 111, 1392
Nemec J. M., Cohen J. G., Ripepi V., Derekas A., Moskalik P., Sesar B., Chadid M., Bruntt H., 2013, ApJ, 773, 181
Pietrzynski G. et al., 2008, AJ, 135, 1993
Romano D., Starkenburg E., 2013, MNRAS, 434, 471
Salaris M., de Boer T., Tolstoy E., Fiorentino G., Cassisi S., 2013, A&A, 559, A57
Schlegel D. J., Finkbeiner D. P., Davis M., 1998, ApJ, 500, 525
Skúladóttir Á., Tolstoy E., Salvadori S., Hill V., Pettini M., Shetrone M. D., Starkenburg E., 2015, A&A, 574, A129
Starkenburg E. et al., 2013, A&A, 549, A88
Stinson G., Seth A., Katz N., Wadsley J., Governato F., Quinn T., 2006, MNRAS, 373, 1074
Tafelmeyer M. et al., 2010, A&A, 524, A58
Tolstoy E. et al., 2004, ApJ, 617, L119
Walker M. G., Mateo M., Olszewski E. W., 2008, ApJ, 688, L75
Yang S.-C., Wagner-Kaiser R., Sarajedini A., Kim S. C., Kyeong J., 2014, ApJ, 784, 76

This paper has been typeset from a TEX/LATEX file prepared by the author.